J Neuropathol Exp Neurol
Vol. 75, No. 2, February 2016, pp. 175–182
doi: 10.1093/jnen/nlv018

ORIGINAL ARTICLE

Altered Levels of Visinin-Like Protein 1 Correspond to Regional Neuronal Loss in Alzheimer Disease and Frontotemporal Lobar Degeneration

Caitlin M. Kirkwood, PhD, Matthew L. MacDonald, PhD, Tadhg A. Schempf, BS, Anil V. Vatsavayi, MD, Milos D. Ikonomovic, MD, Jeremy L. Koppel, MD, Ying Ding, PhD, Mai Sun, PhD, Julia K. Kofler, MD, Oscar L. Lopez, MD, Nathan A. Yates, PhD, and Robert A. Sweet, MD

Abstract

Recent studies have implicated the neuronal calcium-sensing protein visinin-like 1 protein (Vilip-1) as a peripheral biomarker in Alzheimer disease (AD), but little is known about expression of Vilip-1 in the brains of patients with AD. We used targeted and quantitative mass spectrometry to measure Vilip-1 peptide levels in the entorhinal cortex (ERC) and the superior frontal gyrus (SF) from cases with early to moderate stage AD, frontotemporal lobar degeneration (FTLD), and cognitively and neuropathologically normal elderly controls. We found that Vilip-1 levels were significantly lower in the ERC, but not in SF, of AD subjects compared to normal controls. In FTLD cases, Vilip-1 levels in the SF were significantly lower than in normal controls. These findings suggest a unique role for cerebrospinal fluid Vilip-1 as a biomarker of ERC neuron loss in AD.

From the Translational Neuroscience Program (CMK, MLM, TAS, RAS), Department of Psychiatry (CMK, MLM, TAS, MDI, OLL, RAS), Department of Neurology (MDI, OLL, RAS), Department of Pathology (JKK), Biomedical Mass Spectrometry Center (MLM, YD, MS, NAY), Department of Cell Biology (CMK, NAY), University of Pittsburgh Schools of the Health Sciences, Pittsburgh, Pennsylvania; Mental Illness Research, Education, and Clinical Center (RAS), Geriatric Research Education and Clinical Center (MDI), VA Pittsburgh Healthcare System, Pittsburgh, Pennsylvania; Department of Psychiatry (AVV), University of Massachusetts School of Medicine, Worcester, Massachusetts; The Litwin-Zucker Research Center for the Study of Alzheimer's Disease (JLK), The Feinstein Institute for Medical Research (JLK), Manhasset, New York; The Zucker Hillside Hospital (JLK), The North-Shore LIJ Health System, Glen Oaks, New York.

Send correspondence to: Robert Sweet, MD, 3811 O'Hara Street, BST W1645, Pittsburgh, PA 15213; E-mail: sweetra@upmc.edu

This work was supported by grants MH16804 (MLM), AG05133 (OLL), AG014449 (MDI), AG027224 (RAS), and VAPHS grant BX000542 (RAS). The Biomedical Mass Spectrometry Center and UPCI Cancer Proteomics Facility are supported in part by award P30CA047904. The content is solely the responsibility of the authors and does not necessarily represent the official views of the National Institute of Mental Health, the National Institutes of Health, the Department of Veterans Affairs, or the United States Government.

The authors have no biomedical financial interests or potential conflicts of interest to disclose.

Supplementary Data can be found at http://www.jnen.oxfordjournals.org.

Key Words: Alzheimer disease, Frontotemporal lobar degeneration, Human postmortem brain tissue, Visinin-like 1 protein (Vilip-1).

INTRODUCTION

Alzheimer disease (AD) is the leading cause of dementia in the United States affecting more than 5 million people. Clinically, this progressive neurodegenerative disease is characterized by loss of memory, decline in cognitive abilities, and behavioral changes that worsen over time. The 2 major neuropathologic hallmarks of AD are extracellular plaques comprised of the amyloid-β (Aβ) peptide and intracellular neurofibrillary tangles composed of hyperphosphorylated tau protein (1, 2). In addition to accumulating protein aggregates, the brains of patients with AD also exhibit gross anatomical changes, such as atrophy, which results from neuronal cell loss (3, 4).

Several studies have identified the primarily brain-expressed neuronal calcium sensing protein, visinin-like protein 1 (Vilip-1), as a peripheral early stage AD biomarker. Vilip-1 belongs to a large family of calcium-dependent molecular switches and has been shown to modulate receptor trafficking from the cytosol to the plasma membrane. Vilip-1 expression in the brain is neuron-specific (5). Vilip-1 levels have been shown to be elevated in cerebrospinal fluid (CSF) and plasma from individuals with AD compared to cognitively normal control subjects (6). Additionally, higher concentrations of CSF Vilip-1 were predictive of the progression of cognitive decline. Some studies suggested that Vilip-1 CSF elevation phenomenon is specific to AD because no changes were detected in patients with other neurodegenerative disorders such as Lewy body dementia (6, 7). It is not known whether increased Vilip-1 in CSF of AD subjects reflects increased accumulation of this protein in brain parenchyma, or its release due to neuronal cell death (5, 8).

We hypothesized that Vilip-1 alterations in brain tissue are associated with neuronal loss. To test this hypothesis we examined 2 brain regions associated with differing degrees of

neuronal loss in early to moderate stage AD subjects: the entorhinal cortex (ERC) and the superior frontal gyrus (SF) (4, 9–11). We found that Vilip-1 levels were decreased in the ERC and unchanged in the SF in AD subjects compared to normal controls. In contrast, levels of Vilip-1 were significantly lower in the SF of subjects with frontotemporal lobar degeneration (FTLD) compared to controls (12).

MATERIALS AND METHODS

AD and FTLD Patients

AD and FTLD patients were identified through the Brain bank of the Alzheimer Disease Research Center (ADRC) at the University of Pittsburgh using protocols approved by the University of Pittsburgh Institutional Review Board and Committee for Oversight of Research Involving the Dead. Individuals had undergone neurologic, neuropsychological, and psychiatric diagnostic evaluations at successive time points as part of the participation in the Clinical Core of the ADRC, as previously described (13, 14). Neuropathologic assessment and diagnosis were as previously described (15).

Briefly, at autopsy the brains were removed intact, examined grossly, and divided in the midsagittal plane. Postmortem interval (PMI) was recorded. Gray matter samples from the right ERC and SF were dissected and frozen at − 80°C. The left hemibrains were immersion fixed in 10% buffered formalin for at least 1 week, sectioned into 1.0 cm coronal slabs, and sampled according to the Consortium to Establish a Registry for Alzheimer's Disease (CERAD) protocol for the neuropathologic diagnosis of AD. AD pathology was evaluated using modified Bielschowsky silver impregnation and immunohistochemical staining (IHC) for tau and β-amyloid. Neuritic plaque density was assessed according to CERAD criteria (16); distribution of tau pathology was classified according to Braak stages (17). Lewy body pathology was assessed by α-synuclein IHC and classified into brainstem-predominant, limbic and neocortical types following consensus criteria (18). TDP-43 IHC was performed on sections of middle frontal gyrus and mesial temporal lobe, as previously described (15). Sections were evaluated for the absence or presence of TDP-43-positive neuronal cytoplasmic inclusions, neuronal intranuclear inclusions and dystrophic neurites.

Although neuropathologic diagnoses of AD were made according to CERAD criteria, all AD subjects also met NIA-Reagan criteria for intermediate to high probability that their dementia was due to AD lesions (19). Neuropathologic diagnosis of FTLD-TDP, FTLD-FUS, or FTLD-tau was determined following consensus criteria (20–22). When TDP pathology was present in cases that fulfilled diagnostic criteria for another neurodegenerative disease, no distinct diagnosis of FTLD-TDP was rendered, following consensus recommendations (23).

Normal Control Subjects

There were 12 non-demented, neuropathologically normal control cases in the study. Two normal control subject brain specimens were obtained through the ADRC as described above. The remaining 10 normal control subject brain specimens were obtained through the Allegheny County Medical Examiner's Office, with consent obtained from the subjects' next-of-kin. The protocol used to obtain consent was approved by the University of Pittsburgh Institutional Review Board and Committee for Oversight of Research Involving the Dead. An independent committee of experienced clinicians made consensus *Diagnostic and Statistical Manual of Mental Disorders*, *4th Edition* (DSM-IV) diagnoses for each subject, using information obtained from clinical records and structured interviews with surviving relatives. Samples from subjects without any DSM-IV diagnosis (ie, including no diagnosis of a cognitive disorder) were used.

At autopsy, the brains were removed intact, examined grossly, and divided in the midsagittal plane. Samples from the right frontal pole, hippocampus, ERC, and cerebellum were collected, fixed in 4% paraformaldehyde, and processed for hematoxylin and eosin stain, Bielschowsky silver impregnation, amyloid β IHC, and α-synuclein IHC. These sections were reviewed by an experienced neuropathologist and in all cases were determined to be without evidence of any neurodegenerative pathology. The right hemispheres were blocked coronally at 1- to 2-cm intervals and the resultant slabs snap frozen in 2-methyl butane on dry ice, and stored at -80°C. Tissue slabs containing either the SF immediately caudal to the genu of the corpus callosum or the ERC were identified. From these slabs, SF and ERC were removed as single blocks. Gray matter was collected by cutting 40-μm sections and frozen at −80°C.

It is of note that AD and FTLD patient subjects had significantly lower PMIs than normal controls. However, using quantitative Western blot, we previously established the stability of Vilip-1 protein across a 48-hour PMI in a mouse model (Supplementary Data - Fig. 1); therefore, we did not match subjects groups on PMI.

Sample Preparation

Tissue homogenates were prepared from fresh frozen human SF and ERC gray matter. Total protein was extracted using SDS extraction buffer (0.125 M Tris – HCl (pH 7), 2% SDS, and 10% glycerol) at 70°C. Using the bicinchoninic acid assay (Micro BCA^{TM} Protein Assay, Pierce, Rockford, IL), protein concentration was measured. A pooled technical replicate sample composed of homogenate aliquots from all subjects was also prepared for each experiment (SF and ERC). Twenty μg of total protein from the gray matter homogenate or pooled sample was mixed with Lysine $^{13}C_6$ Stable Isotope Labeled Neuronal Proteome Standard ($^{13}C_6$ STD; 20 μg) for on-gel trypsin digestion. To evenly distribute AD, FTLD, and normal control subjects throughout preparation, on-gel digestion, and analysis, samples were organized in a block distribution. For the SF experiment, each block was composed of 7 subjects and 1 pooled technical replicate, for a total of 12 blocks. For the ERC experiment, each block was also composed of 7 subjects and 1 pooled technical replicate, for a total of 4 blocks. Each block was run on a single 10-well

4%–12% BisTris gel with 2 SeeBlue® Plus2 Pre-stained Protein Standards. On-gel trypsin digestion was performed as previously described (24), with samples run 4 cm into the gel and divided into 2 fractions (above and below 65 kDa).

Liquid Chromatography-Selected Reaction Monitoring/Mass Spectrometry

Vilip-1 and microtubule-associated protein 2 (MAP2) peptides were selected for analysis based on the presence of a lysine, the amino acid labeled in the $^{13}C_6$ STD, and 100% homology across mouse and human sequences (determined by Uniprot BLAST search). Five peptide sequences were identified from the Vilip-1 protein for quantification as indicated as underlined text in the following Vilip-1 amino acid sequence:

MGKQNSKLAPEVMEDLVKSTEFNEHELKQWYK GFLKDCPSGRLNLEEFQQLYVKFFPYGDASKFAQHA FRTFDKNGDGTIDFREFICALSITSRGSFEQKLNWAFN MYDLDGDGKITRVEMLEIIEAIYKMVGTVIMMKMNE DGLTPEQRVDKIFSKMDKNKDDQITLDEFKEAAKSDP SIVLLLQCDIQK

Additionally, 2 peptide sequences were identified from the neuronal integrity marker, MAP2, for quantification to assess neuronal loss (Supplementary Data - Fig. 2A).

Liquid chromatography-selected reaction monitoring/mass spectrometry (LC-SRM/MS) analyses were conducted as previously described (24). In brief, peptide peaks were detected using a TSQ Quantiva triple stage quadrupole mass spectrometer (Thermo Scientific) with an UltiMate 3000 Nano LC Systems (Thermo Scientific). Two µl (~1 µg protein) of sample was loaded/desalted on a PepMap100 Nano-Trap column (Thermo Scientific) at 8 µl/minute for 2 minutes and separated on a Reprosil-pur 3-µm PicoChip column (New Objective, Woburn, MA) at 400 nl/minute over a 20-minute gradient from 2%–35% mobile phase B (Acetonitrile containing 0.1% formic acid). SRM transitions were timed using 1.5-minute retention windows. Transitions were monitored, allowing for a cycle time of 1 second, resulting in a dynamic dwell time, never falling below 2 mseconds. The MS instrument parameters were as follows: capillary temperature 275°C; spray voltage 1100 V; and a collision gas of 1.4 mTorr (argon). The resolving power of the instrument was set to 0.7 Da (full width half maximum) for the first and third quadrupole. All samples were analyzed in triplicate. Using Skyline, integrated peak areas for both "light" human peptides and the "heavy" $^{13}C_6$ STD peptides were calculated for each of the peptide sequences. The light:heavy integrated area ratio was calculated to obtain peptide measures using multiple transitions per peptide. We have previously demonstrated that this approach yields high reproducibility and linearity of measurement across several orders of magnitude of peptide abundance (24), and observed similar sensitivity for detection of Vilip-1 (Supplementary Data - Fig. 2B-F). Coefficients of variation for Vilip-1 and MAP2 peptides in the current experiment are shown in Supplementary Data - Table 1.

Measurement of Soluble Aβ and Phospho-tau by Sandwich Enzyme-Linked Immunosorbent Assay

Levels of soluble Aβ1-40 and Aβ1-42 and of tau protein had been previously determined in SF from a subset of study subjects (25, 26). See Supplemental Methods for additional details.

Statistical Analysis

All light:heavy ratios were log2 transformed for statistical analysis. Replicate peptide values were averaged prior to analysis. Assessment of demographic, clinical, and pathological differences between groups was performed using analysis of variance (ANOVA), t-tests, or $\chi 2$ tests. Initial comparison of Vilip-1 and MAP2 peptide levels between AD subjects and normal control subjects used two-sample T-tests for both the ERC and SF regions. A repeated measure two-way ANOVA was employed to evaluate the brain region by diagnosis interaction with correlations between the 2 measurements (in ERC and SF regions) from the same sample being accounted for. In the SF region, ANCOVA was used to assess whether demographic, clinical, and pathological subgroups affected individual Vilip-1 and MAP2 peptide levels.

RESULTS

Alterations in Vilip-1 Levels in ERC and SF Cortex From Controls, AD, and FTLD Cases

Vilip-1 levels were assessed in ERC and SF of 12 AD cases and 12 cognitively normal controls (Table 1). Vilip-1

TABLE 1. Subjects of Cohort 1

Variable	Alzheimer Disease (n = 12)	Control (n = 12)
Age (years)[a]	84.5 ± 8.9	70.7 ± 9.4
Range (years)	71–101	56–89
Sex		
Male	5 (42)	8 (67)
Female	7 (58)	4 (33)
Postmortem interval (hours)[a]	5.1 ± 2.9	12.2 ± 5.9
Range (hours)	2–10	4–20
Age of onset (years)	76.0 ± 9.0	
Range (years)	63– 90	
Duration of Illness (years)	7.9 ± 3.0	
Range (years)	4–13	
α-synuclein		
Negative	12 (100)	
Brainstem/Transitional	0 (0)	
Neocortical	0 (0)	
Braak		
4	3 (25)	
5	9 (75)	

Mean values ± SD or number of subjects with percentage of group in parentheses.

[a]Indicates groups differ significantly on these variables.

peptide levels in the ERC were significantly decreased in AD cases compared to cognitively normal controls (Fig. 1; Table 2). However, in AD SF, Vilip-1 levels were not significantly different from cognitively normal controls. The above pattern was found for all 5 Vilip-1 peptides, and for all of them in the region by diagnosis interaction reached significance (Table 2).

The observed decrease in Vilip-1 levels selectively in the ERC from AD cases suggested that it might be related to neuronal loss. We conducted 2 further analyses. First, we evaluated Vilip-1 peptide levels in the SF of FTLD subjects (Table 3), compared to control cases and to an expanded cohort of AD cases. SF Vilip-1 levels in FTLD were significantly lower than in cognitively normal controls and AD cases for all peptides (Fig. 2; Table 4).

Next, we assessed levels of MAP2, a marker that is reduced by neuron loss (27) in the ERC and SF of all cases. MAP2 levels were significantly decreased in ERC of AD cases compared to normal controls (all $p < 0.001$; Table 5), and decreases in the ERC exceeded those in the SF of these cases. In the SF, the magnitude of reduction in MAP2 levels was greater in FTLD than in AD (Table 6). Similarly, within the SF of AD cases, Vilip-1 levels and MAP2 levels were significantly correlated (Supplementary Data - Fig. 3). In contrast, Vilip-1 levels in the SF of AD cases did not correlate with measures of fibrillar tau, soluble total tau or phosphorylated tau, soluble $A\beta_{1\text{-}42}$, soluble $A\beta_{1\text{-}40}$, Braak Stage, or comorbid Lewy body pathology (Supplementary Data - Fig. 3).

Role of Vilip-1 in Aβ-induced Neuronal Death *In Vitro*

A previous study found that overexpression of Vilip-1 in PC12 cells increased cell death in response to a calcium challenge (28), suggesting that Vilip-1 may not be only a marker of neuronal death in AD, but may contribute actively to the process. To evaluate this possibility, we investigated whether altering Vilip-1 levels impacted Aβ-induced neuronal death in Vilip-1 heterozygous and wild type mice primary neuronal cultures. Soluble $A\beta_{1\text{-}42}$ exposure led to robust increases in cell death rates in cultures derived from both Vilip-1 heterozygous and wild type mice. We saw no significant difference in cell death rates following soluble $A\beta_{1\text{-}42}$ exposure between heterozygous Vilip-1 and wild-type genotypes (Supplementary Data - Fig. 4).

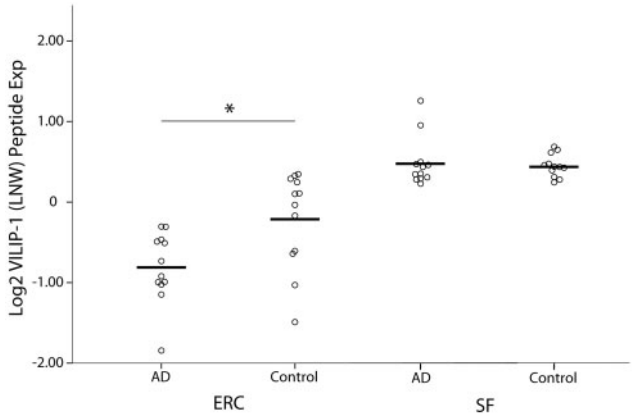

FIGURE 1. Log_2-transformed expression ratios of a representative peptide, Vilip-1 (LNW) in the entorhinal cortex (ERC) and the superior frontal gyrus (SF) comparing Alzheimer disease (AD) patients ($n = 12$) and cognitively normal control subjects ($n = 12$). *Indicates $p < 0.05$. See Table 2 for statistical tests used.

Vilip-1 Levels in SF of AD Cases and Clinical Indicators of Disease Severity

Because CSF levels of Vilip-1 are predictive of more rapid cognitive decline, we examined SF Vilip-1 levels in the expanded AD cohort to assess whether indicators of greater disease severity would be associated with reduced SF Vilip-1 in AD. No association was observed between Vilip-1 levels and Mini-Mental State Examination (MMSE) score at death, or between Vilip-1 levels and the presence of psychosis (an indicator of a more rapidly progressive AD subgroup [25]). Nor did SF Vilip-1 levels correlate with age at death, age of disease onset, and duration of illness.

DISCUSSION

We evaluated the hypothesis that Vilip-1 is altered in AD and associated with neurodegeneration by assessing Vilip-1 protein levels in 2 different brain regions with varying degrees of neuronal loss. We found Vilip-1 levels were decreased in the ERC of AD subjects, an area with greater neuronal loss even at early stages of the disease. However, in the SF, an area with comparatively less neuronal loss in early to moderate disease stages, Vilip-1 levels in AD did not differ from those in normal controls. In contrast, Vilip-1 levels in the SF were decreased in FTLD subjects, which have neuronal loss in the frontal and temporal lobes. Additionally, in an expanded group of AD subjects, lower Vilip-1 levels in the SF correlated with lower levels of MAP2, but did not associate with other neuropathologic measures including Braak stage, total and phosphorylated tau levels, soluble $A\beta_{1\text{-}42}$, soluble $A\beta_{1\text{-}40}$, and Lewy body pathology. These findings provide evidence that Vilip-1 is altered in AD and may be more closely associated with neuronal loss than with upstream pathologies such as Aβ and phosphorylated tau accumulation.

Recent studies have identified a potential role for Vilip-1 as a biomarker in AD. CSF and plasma Vilip-1 levels have been shown to be elevated in mild cognitive impairment and AD compared to normal control subjects (6, 29, 30). Additionally, Vilip-1 CSF levels were predictive of subsequent cognitive decline, as higher Vilip-1 levels in CSF indicated a more rapid deterioration in cognitive performance (29, 31, 32). While CSF Vilip-1 levels are elevated in AD, our findings, which are the first reported quantitative levels of Vilip-1 in human brain tissue, indicate decreased ERC and unchanged SF Vilip-1 protein levels in early to moderate AD stages. The most parsimonious explanation of this combination of CSF, ERC, and SF findings is that Vilip-1 is released upon

TABLE 2. Summary of Vilip-1 Peptide Expression in ERC and SF Brain Regions and the Effect of Region by Diagnosis From Cohort 1

	ERC			SF			Region by Diagnosis	
Peptide	**AD:Control**	**t, df**	**p Value[a]**	**AD:Control**	**t, df**	**p Value**	**F, df**	**p Value[a]**
STE	0.680	−2.618, 22	0.016	1.075	0.858, 22	0.400	7.283, 1, 44	0.010
LNL	0.694	−2.322, 22	0.030	1.076	0.944, 22	0.355	6.251, 1, 44	0.016
LNW	0.661	−2.788, 22	0.011	1.027	0.399, 22	0.694	7.309, 1, 44	0.010
VEM	0.653	−2.621, 22	0.016	1.033	0.475, 22	0.639	6.770, 1, 44	0.013
SDP	0.676	−2.480, 22	0.021	0.972	−0.366, 22	0.718	4.294, 1, 44	0.044

AD, Alzheimer disease; ERC, entorhinal cortex; SF, superior frontal gyrus; n = 12; cognitively normal control; n = 12 AD).

[a]All values in column indicate significance ($p < 0.05$).

TABLE 3. Descriptive Information of Subjects in Cohort 2

Variable	**AD n = 58**	**FTLD n = 10[b]**
Age (years)[a]	84.2 ± 7.0	74.7 ± 10.4
Range (years)	68–101	62–90
Sex		
Male	29 (50)	4 (40)
Female	29 (50)	6 (60)
Postmortem interval (hours)	6.1 ± 3.4	6.2 ± 2.3
Range (hours)	2–17	4–20
Age of onset (years)*	75.9 ± 7.0	64.7 ± 10.3
Range (years)	57–90	47–89
Duration of Illness (years)	8.2 ± 3.3	10.0 ± 4.2
Range (years)	2–18	6–18
α-synuclein		
Negative	30 (52)	
Brainstem/Transitional	15 (26)	
Neocortical	13 (22)	
Braak		
3	6 (10)	
4	20 (35)	
5	32 (55)	

AD, Alzheimer disease; FTLD, frontotemporal lobar degeneration.

This expanded cohort contains all subjects from Cohort 1 with an additional 46 AD subjects and 10 FTLD Subjects.

[a]Indicates groups differ significantly on these variables.

[b]FTLD subtypes: TDP-43, n = 4; Tau, n = 6.

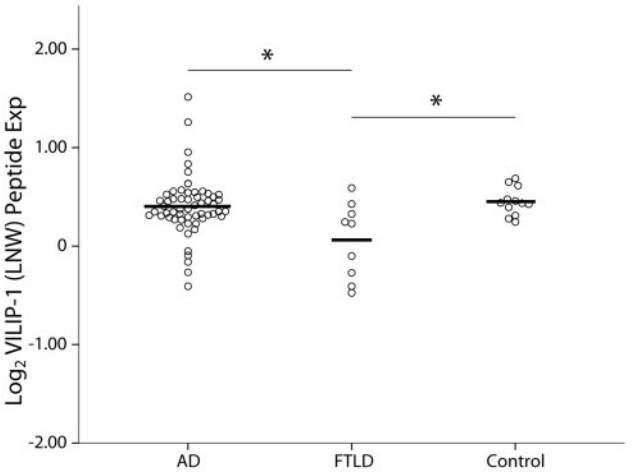

FIGURE 2. Log_2-transformed expression ratios of a representative peptide, Vilip-1 (LNW) in the superior frontal gyrus comparing an expanded cohort of patients with Alzheimer disease (AD) (n = 58), frontotemporal lobar degeneration (FTLD) subjects (n = 10), and cognitively normal control subjects (n = 12). *Indicates $p < 0.05$. See Table 4 for statistical tests used.

neuronal death (8), and that such release from degenerating ERC neurons into interstitial fluid is sufficient to influence the CSF compartment sampled by lumbar puncture.

The impact of the ERC on CSF levels could reflect the overall greater extent of neuron loss in this region in AD. Neuronal loss occurs in the ERC of AD subjects and the SF of FTLD subjects (4, 12). Conversely, despite reductions in cortical volume, stereological studies have found limited loss of neurons within the frontal cortex of subjects with mild to moderate AD (10, 11). Although neuronal counts in the ERC and SF of our subjects were not available, we assessed MAP2 peptide levels as a confirmatory measure to assess neuronal loss. MAP2 is a neuron-specific protein that interacts with microtubules and the cell cytoskeleton (33). Because it is among the most vulnerable cytoskeletal proteins, MAP2 immunoreactivity is lost in neuronal death (27). We found that MAP2 levels were significantly decreased in the ERC of AD subjects compared to normal controls. MAP2 levels were also reduced, albeit to a lesser extent, in the SF of AD subjects compared to normal controls. However, in FTLD subjects the magnitude of MAP2 reduction was greater, consistent with a larger amount of neuronal loss in FTLD compared to AD in this region. Conversely, our lab has previously reported that MAP2 peptide levels are unchanged in auditory cortex of schizophrenia subjects, a region without neuronal loss in that disease (34). Finally, although there was no reduction in Vilip-1 levels in the SF in AD subjects as a group, within subject Vilip-1 and MAP2 levels were correlated.

A number of other factors may also lead the ERC to have a greater impact on CSF Vilip-1 levels than SF. First, proximity of the ERC to the ventricular system could impact protein diffusion and penetration into the CSF. A dual neuroimaging-CSF study investigating how brain Aβ deposition is reflected in the CSF, correlated carbon-11-labeled Pittsburgh Compound B, which binds fibrillar Aβ deposits in the brain, with CSF $A\beta_{1\text{-}42}$ concentrations in 30 patients with probable AD. They found that the relationship between CSF Aβ concentrations and amyloid load in the brain were strongest within brain regions surrounding the ventricles, suggesting that CSF protein levels may chiefly reflect pathology localized to brain regions in the vicinity of the ventricular system (35). Notably, this idea of access via proximity of the affected brain region to the ventricle is consistent with the anatomy of our observed Vilip-1 reductions in brain regions with significant neuronal loss. The hippocampus, which is anatomically juxtaposed to the ERC, is located in the temporal lobe, medial to the inferior horn of the lateral ventricle. The hippocampal-CSF interface runs the entire length of lateral ventricle in each hemisphere of the brain, while the frontal cortex is located relatively far from the ventricular system (36). In addition to proximity, MRI studies have demonstrated the breakdown of the ventricular lining in AD, rendering it more accessible to proteins in the local interstitium (37), which could include Vilip-1 released upon neuronal death in the ERC.

Given the correlation of Vilip-1 with a marker of neuronal death, an important question is whether Vilip-1 merely reflects neuron death, or in some way contributes to that process in AD. A previous study had found that Vilip-1 overexpression in pheochromocytoma cells leads to increased Ca^{2+}-mediated cell death (28). However, because we found decreased, not increased, Vilip-1 in AD (and no evidence of increased Vilip-1 in a mouse model of Aβ overproduction, Supplementary Data - Fig. 5), we chose to evaluate whether Vilip-1 reductions altered the magnitude of Aβ-mediated cortical neuronal death. We found no evidence of an effect of Vilip-1 levels on this process. Although these findings should be subject to further replication, they suggest Vilip-1 is unlikely involved in an AD-specific death mechanism in cortical neurons and more likely serves solely as a nonspecific marker of neuron death.

TABLE 4. Summary of Vilip-1 Peptide Expression Diagnosis Differences From Expanded Alzheimer Disease Subject Cohort Group

	AD vs. Control		AD vs. FTLD		FTLD vs. Control	
Peptide	AD: Control	P Value	AD: FTLD	p Value[a]	FTLD: Control	p Value[a]
STE	1.024	0.161	1.335	0.002	0.767	< 0.001
LNL	0.746	0.478	1.300	< 0.001	0.773	< 0.001
LNW	0.984	0.592	1.254	0.002	0.784	0.003
VEM	0.996	0.245	1.376	0.017	0.724	0.003
SDP	0.934	0.618	1.600	0.002	0.584	0.004

AD, Alzheimer disease; FTLD, frontotemporal lobar degeneration.

AD subject group (n = 58); FTLD subject group (n = 10); cognitively normal controls (n = 12)

[a]All values in column indicate significance ($p < 0.05$).

TABLE 5. Summary of MAP2 Peptide Expression in Entorhinal Cortex and Superior Frontal Gyrus Regions and the Effect of Region by Diagnosis in Cohort 1

MAP2 Peptide	Entorhinal cortex			Superior frontal gyrus			Region by Diagnosis	
	AD:Control	t, df	p Value	AD:Control	t, df	p Value	F, df	p Value
LIN	0.242	4.638, 21	< 0.001*	0.63	2.106, 22	0.047*	7.792, 22	0.011[a]
DLA	0.299	5.119, 21	< 0.001*	0.805	1.375, 22	0.183	19.993, 22	< 0.001[a]

AD, Alzheimer disease; MAP2, microtubule-associated protein 2.

Cohort 1: AD, n = 12; cognitively normal controls, n = 12.

[a]Significant values ($p < 0.05$).

TABLE 6. Summary of MAP2 Peptide Expression Diagnosis Differences From Expanded Cohort Group

MAP-2 Peptide	AD vs. Control		FTLD vs. Control		AD vs. FTLD	
	AD:Control	p Value	FTLD:Control	p Value	AD:FTLD	p Value
LIN	0.554	0.010[a]	0.358	< 0.001[a]	1.439	0.054
DLA	0.729	0.065	0.507	< 0.001[a]	1.549	0.013[a]

AD, Alzheimer disease; FTLD, frontotemporal lobar degeneration; MAP-2, microtubule-associated protein 2.

AD subject group (n = 58); FTLD subject group (n = 10); cognitively normal controls (n = 12).

[a]Indicates significant values ($p < 0.05$).

Previous reports have qualitatively described Vilip-1 associating with other AD pathologies, like neuritic plaques and neurofibrillary tangles in the neocortex (38). Others have indicated that Vilip-1 may play an active role in tau phosphorylation (28). However, we found that Vilip-1 levels in the SF did not correlate with any other measures of amyloid or tau pathology, including Braak stage, soluble $A\beta_{1\text{-}42}$, $A\beta_{1\text{-}40}$, total or phosphorylated tau levels. The discrepancy between our findings and previous work may be in part due to the approach used. We used quantitative LC-SRM/MS of gray matter brain homogenate to measure total levels of Vilip-1 peptide in brain tissue, an approach that allowed for simultaneous measurement and quantification of five Vilip-1 peptides with high precision and reproducibility. Peptide detection was linear and over repeated runs we observed low variability in peptide measures. Similarly, we used highly specific ELISA (enzyme-linked immunosorbent assays) to measure soluble $A\beta_{1\text{-}42}$, $A\beta_{1\text{-}40}$ and total and phosphorylated tau. In contrast, the prior study indicating an association of Vilip-1 with plaque and tangle pathology used qualitative IHC (38). Alternatively, we may have failed to detect a correlation between Vilip-1 and neurofibrillary pathology due to the limited range of this pathology in the SF at the Braak stages (3–5) studied, and/or the limited extent of neuronal loss in this region at these stages. In fact, our principal finding, that Vilip-1 levels are decreased within the ERC, but not SF, of AD subjects, can be seen as strong evidence of a correlation of Vilip-1 loss with neurofibrillary pathology, as the ERC has substantially greater neurofibrillary pathology than the SF at Braak stages 3 to 5.

A noteworthy discrepancy exists between the current findings of reduced SF Vilip-1 levels in FTLD in comparison to AD and control subjects and prior CSF findings that Vilip-1 levels in non-AD dementia subjects, including individuals clinically diagnosed with frontotemporal dementia and Lewy body dementia were lower than in AD, and no different from control subjects (6). Although this discrepancy could arise from the increased access of ERC to the CSF in AD, without having CSF measurements from a neuropathologically verified population of FTLD subjects, it remains possible that CSF Vilip-1 levels are changed in this neurodegenerative disorder. Alternatively, future postmortem studies involving larger numbers of FTLD subjects of each pathologic subtype and including more subjects with short durations of illness may reveal greater variability in the degree of Vilip-1 reductions than seen in the current study.

A potential limitation of this study was the significantly younger normal control group. We opted to utilize a neuropathologically normal control group, as previous Western blot data from our laboratory (not shown) indicated decreased levels of Vilip-1 in controls with asymptomatic comorbid neuropathologies such as mesial temporal sclerosis and cerebrovascular disease. Additionally, selection of age-matched control subjects is complicated, as many biomarker and neuroimaging studies have demonstrated that amyloid deposition in AD begins decades prior to the emergence of cognitive symptoms (39, 40). Thus to obtain neuropathologically normal subjects, our control group was of younger age. Despite these obstacles, several observations make it unlikely that age is associated with the alterations we observed in Vilip-1. First, it would be difficult to explain an age effect that led to differential expression of Vilip-1 in the ERC, but not SF, of the same subjects. Second, we have shown (using microarray analysis of cognitively normal adults) that Vilip-1 mRNA is unaffected by age across the adult lifespan (41). Finally, our FTLD subjects were substantially younger than our AD cohort yet still had significantly reduced Vilip-1 protein levels compared to controls. Another potential confound in human tissue studies is matching normal control subjects as closely as possible on PMI. Our study included AD with significantly lower PMIs than normal controls; however, we previously established the stability of Vilip-1 protein across a 48-hour PMI in a mouse model, a much greater range than in the current study. Moreover, as for age difference, it would be difficult to reconcile a PMI effect with differential expression of Vilip-1 only in the ERC, but not SF, of the same subject pairs. Finally, there was a non-significant trend towards a greater proportion of male control subjects. However, SF and ERC Vilip-1 levels did not differ by sex, nor were there any sex x diagnosis interactions, and there was no effect of sex on the differential expression of Vilip-1 in the ERC, but not SF (data not shown).

In summary, we found that Vilip-1 levels in the ERC, but not the SF, were significantly lower in AD subjects compared to normal controls. In FTLD cases, Vilip-1 levels in the SF were significantly lower than in normal controls. Our findings suggest that CSF measurement of Vilip-1 can serve as a direct *in vivo* index of ERC (and possibly hippocampal) neuron death in early to middle stages of AD. Currently no such index exists, although medial temporal atrophy, assessable on brain imaging, certainly includes an indirect assessment of neuron loss in this region. This interpretation would justify expanded investigation of Vilip-1 as a CSF biomarker in AD and evaluation of its utility as an index of neuronal survival (neuroprotection) during intervention studies in humans and in appropriate animal models.

ACKNOWLEDGMENTS

The research complied with Institutional Animal Care and Use Committee protocols. The authors thank Dr. Susan Erickson for her assistance with data generation. The content is solely the responsibility of the authors and does not necessarily represent the official views of the National Institute of Mental Health, the National Institutes of Health, the Department of Veterans Affairs, or the United States Government.

REFERENCES

1. Selkoe DJ. Alzheimer disease: Mechanistic understanding predicts novel therapies. Ann Intern Med 2004;140:627–38
2. Ballatore C, Lee VM, Trojanowski JQ. Tau-mediated neurodegeneration in Alzheimer's disease and related disorders. Nat Rev Neurosci 2007;8:663–72
3. Ingelsson M, Fukumoto H, Newell KL, et al. Early Abeta accumulation and progressive synaptic loss, gliosis, and tangle formation in AD brain. Neurology 2004;62:925–31
4. Gomez-Isla T, Price JL, McKeel DW, Jr., et al. Profound loss of layer II entorhinal cortex neurons occurs in very mild Alzheimer's disease. J Neurosci 1996;16:4491–4500

5. Bernstein HG, Baumann B, Danos P, et al. Regional and cellular distribution of neural visinin-like protein immunoreactivities (VILIP-1 and VILIP-3) in human brain. J Neurocytol 1999;28:655–62
6. Tarawneh R, D'Angelo G, Macy E, et al. Visinin-like protein-1: Diagnostic and prognostic biomarker in Alzheimer disease. Ann Neurol 2011;70: 274–85
7. Luo X, Hou L, Shi H, et al. CSF levels of the neuronal injury biomarker visinin-like protein-1 in Alzheimer's disease and dementia with Lewy bodies. J Neurochem 2013;127:681–90
8. Laterza OF, Modur VR, Crimmins DL, et al. Identification of novel brain biomarkers. Clin Chem 2006;52:1713–21
9. Regeur L, Jensen GB, Pakkenberg H, et al. No global neocortical nerve cell loss in brains from patients with senile dementia of Alzheimer's type. Neurobiol Aging 1994;15:347–52
10. Bussiere T, Gold G, Kovari E, et al. Stereologic analysis of neurofibrillary tangle formation in prefrontal cortex area 9 in aging and Alzheimer's disease. Neuroscience 2003;117:577–92
11. Giannakopoulos P, Hof PR, Kovari E, et al. Distinct patterns of neuronal loss and Alzheimer's disease lesion distribution in elderly individuals older than 90 years. J Neuropathol Exp Neurol 1996;55:1210–20
12. Cairns NJ, Brannstrom T, Khan MN, et al. Neuronal loss in familial frontotemporal dementia with ubiquitin-positive, tau-negative inclusions. Exp Neurol 2003;181:319–26
13. Lopez OL, Becker JT, Chang YF, et al. The long-term effects of conventional and atypical antipsychotics in patients with probable Alzheimer's disease. Am J Psychiatr 2013;170:1051–8
14. Sweet RA, Hamilton RL, Lopez OL, et al. Psychotic symptoms in Alzheimer's disease are not associated with more severe neuropathologic features. Int Psychogeriatr 2000;12:547–58
15. Vatsavayi AV, Kofler J, Demichele-Sweet MA, et al. TAR DNA-binding protein 43 pathology in Alzheimer's disease with psychosis. Int Psychogeriatr 2014;26:987–94
16. Mirra SS, Heyman A, McKeel D, et al. The Consortium to Establish a Registry for Alzheimer's Disease (CERAD). Part II. Standardization of the neuropathologic assessment of Alzheimer's disease. Neurology 1991;41:479–86
17. Braak H, Alafuzoff I, Arzberger T, et al. Staging of Alzheimer disease-associated neurofibrillary pathology using paraffin sections and immunocytochemistry. Acta Neuropathol 2006;112:389–404
18. McKeith IG, Dickson DW, Lowe J, et al. Diagnosis and management of dementia with Lewy bodies: Third report of the DLB Consortium. Neurology 2005;65:1863–72
19. Hyman BT, Trojanowski JQ. Consensus recommendations for the postmortem diagnosis of Alzheimer disease from the National Institute on Aging and the Reagan Institute Working Group on diagnostic criteria for the neuropathological assessment of Alzheimer disease. J Neuropath Exp Neurol 1997;56:1095–7
20. Mackenzie IR, Neumann M, Bigio EH, et al. Nomenclature and nosology for neuropathologic subtypes of frontotemporal lobar degeneration: an update. Acta Neuropathol 2010;119:1–4
21. Mackenzie IR, Neumann M, Baborie A, et al. A harmonized classification system for FTLD-TDP pathology. Acta Neuropathol 2011;122:111–13
22. Cairns NJ, Bigio EH, Mackenzie IR, et al. Neuropathologic diagnostic and nosologic criteria for frontotemporal lobar degeneration: Consensus of the Consortium for Frontotemporal Lobar Degeneration. Acta Neuropathol 2007;114:5–22
23. Mackenzie IR, Neumann M, Bigio EH, et al. Nomenclature for neuropathologic subtypes of frontotemporal lobar degeneration: consensus recommendations. Acta Neuropathol 2009;117:15–18
24. MacDonald ML, Ciccimaro E, Prakash A, et al. Biochemical fractionation and stable isotope dilution liquid chromatography-mass spectrometry for targeted and microdomain-specific protein quantification in human postmortem brain tissue. Mol Cell Proteomics 2012;11: 1670–81
25. Murray PS, Kirkwood CM, Gray MC, et al. beta-Amyloid 42/40 ratio and kalirin expression in Alzheimer disease with psychosis. Neurobiol Aging 2012;33:2807–16
26. Koppel J, Acker C, Davies P, et al. Psychotic Alzheimer's disease is associated with gender-specific tau phosphorylation abnormalities. Neurobiol Aging 2014;35:2021–28
27. Huh JW, Raghupathi R, Laurer HL, et al. Transient loss of microtubule-associated protein 2 immunoreactivity after moderate brain injury in mice. J Neurotrauma 2003;20:975–84
28. Schnurra I, Bernstein HG, Riederer P, et al. The neuronal calcium sensor protein VILIP-1 is associated with amyloid plaques and extracellular tangles in Alzheimer's disease and promotes cell death and tau phosphorylation in vitro: a link between calcium sensors and Alzheimer's disease? Neurobiol Dis 2001;8:900–909
29. Mroczko B, Groblewska M, Zboch M, et al. Evaluation of visinin-like protein 1 concentrations in the cerebrospinal fluid of patients with mild cognitive impairment as a dynamic biomarker of Alzheimer's disease. J Alzheimers Dis 2015;43:1031–37
30. Lee JM, Blennow K, Andreasen N, et al. The brain injury biomarker VLP-1 is increased in the cerebrospinal fluid of Alzheimer disease patients. Clin Chem 2008;54:1617–23
31. Tarawneh R, Lee JM, Ladenson JH, et al. CSF VILIP-1 predicts rates of cognitive decline in early Alzheimer disease. Neurology 2012;78: 709–19
32. Fagan AM, Xiong C, Jasielec MS, et al. Longitudinal change in CSF biomarkers in autosomal-dominant Alzheimer's disease. Sci Transl Med 2014;6:226ra230
33. Dehmelt L, Halpain S. The MAP2/Tau family of microtubule-associated proteins. Genome Biol 2005;6:204
34. Shelton MA, Newman JT, Gu H, et al. Loss of microtubule-associated protein 2 immunoreactivity linked to dendritic spine loss in schizophrenia. Biol Psychiatry 2015;78:374–85
35. Grimmer T, Riemenschneider M, Forstl H, et al. Beta amyloid in Alzheimer's disease: Increased deposition in brain is reflected in reduced concentration in cerebrospinal fluid. Biol Psychiatry 2009;65:927–34
36. Johanson CE, Duncan JA, Stopa EG, et al. Enhanced prospects for drug delivery and brain targeting by the choroid plexus-CSF route. Pharm Res 2005;22:1011–37
37. Scheltens P, Barkhof F, Leys D, et al. Histopathologic correlates of white matter changes on MRI in Alzheimer's disease and normal aging. Neurology 1995;45:883–88
38. Braunewell K, Riederer P, Spilker C, et al. Abnormal localization of two neuronal calcium sensor proteins, visinin-like proteins (vilips)-1 and -3, in neocortical brain areas of Alzheimer disease patients. Dement Geriatr Cogn Disord 2001;12:110–16
39. Tosun D, Joshi S, Weiner MW. Neuroimaging predictors of brain amyloidosis in mild cognitive impairment. Ann Neurol 2013;74:188–98
40. Resnick SM, Sojkova J, Zhou Y, et al. Longitudinal cognitive decline is associated with fibrillar amyloid-beta measured by [11C]PiB. Neurology 2010;74:807–15
41. Lin CW, Chang LC, Tseng GC, et al. VSNL1 co-expression networks in aging include calcium signaling, synaptic plasticity, and Alzheimer's disease pathways. Front Psychiatry 2015;6:30